

Classical capacity of Gaussian thermal memory channels

G. De Palma,^{1,2} A. Mari,¹ and V. Giovannetti¹¹*NEST, Scuola Normale Superiore and Istituto Nanoscienze-CNR, I-56127 Pisa, Italy*²*INFN, Pisa, Italy*

(Received 7 April 2014; published 10 October 2014)

The classical capacity of phase-invariant Gaussian channels has been recently determined under the assumption that such channels are memoryless. In this work we generalize this result by deriving the classical capacity of a model of quantum memory channel, in which the output states depend on the previous input states. In particular we extend the analysis of Lupo *et al.* [*Phys. Rev. Lett.* **104**, 030501 (2010) and *Phys. Rev. A* **82**, 032312 (2010)] from quantum limited channels to thermal attenuators and thermal amplifiers. Our result applies in many situations in which the physical communication channel is affected by nonzero memory and by thermal noise.

DOI: [10.1103/PhysRevA.90.042312](https://doi.org/10.1103/PhysRevA.90.042312)

PACS number(s): 03.67.Hk, 05.40.Ca, 42.50.-p, 89.70.-a

I. INTRODUCTION

Given a physical device acting as a quantum communication channel [1,2], an important problem in quantum information theory is to determine the optimal rate of classical information that can be sent through the channel assuming that one is allowed to use arbitrary quantum encoding and decoding strategies possibly involving multiple uses of the transmission line (*channel uses*). The maximum achievable rate is the *classical capacity* associated to the quantum channel [2–4]. A simple closed formula for this quantity does not exist, since typically it is not easy to see whether entangled input states will improve the communication rate. Still it is possible to prove [2] that if no memory effects are tampering with the communication line (i.e., if the noise affecting the communication acts identically and independently on subsequent channel uses) the classical capacity of the setup can be expressed as the following limit:

$$C(\Phi) = \lim_{n \rightarrow \infty} \frac{1}{n} \chi(\Phi^{\otimes n}), \quad (1)$$

where Φ is the (completely positive, trace-preserving) mapping characterizing the input-output relations of a single channel use, and where $\chi(\Phi^{\otimes n})$ is the Holevo information of n channel uses, which is defined through the identity

$$\chi(\Phi) = \sup_{\mu} \left[S \left(\int \Phi(\rho) d\mu(\rho) \right) - \int S(\Phi(\rho)) d\mu(\rho) \right], \quad (2)$$

the supremum being taken over all probability measures μ on the space of the density matrices ρ of the system, and S being the von Neumann entropy, i.e., $S(\rho) = -\text{Tr}[\rho \ln \rho]$.

Most real communication media are based on electromagnetic signals and are well described within the framework of quantum Gaussian channels [5–7]. The most relevant class is constituted by phase-invariant channels such as attenuators and amplifiers. Such channels reduce or increase the amplitude of the signal and, at the same time, they add a certain amount of Gaussian noise which depends on the vacuum or thermal fluctuations of the environment. Recently the proof of the minimum output entropy conjecture [8,9] has allowed the determination of the exact classical capacities of these channels [10] and the respective strong converse theorems [11], under the crucial assumption of their memoryless behavior. One of

the key points of the proof is the additivity of the χ capacity of a memoryless phase-invariant Gaussian channel:

$$\chi(\Phi^{\otimes n}) = n\chi(\Phi), \quad (3)$$

which trivializes the limit in (1). Realistic communication lines, however, if used at high rates (larger than the relaxation time of the environment), may exhibit memory effects in which the output states are influenced by the previous input signals [12–15]. In other words, the noise introduced by the channel instead of being independent and identically distributed can be correlated with the previous input states preventing one from expressing the input-output mapping of n successive channel uses as a simple tensor product $\Phi^{\otimes n}$ and hence from using Eq. (1). As a matter of fact since the capacity is defined asymptotically in the limit of many repeated channel uses, memory effects will affect the optimal information rate and the optimal coding strategies. A characterization of *quantum memory channels* can be found in Refs. [16–18], while generalizations to infinite dimensional bosonic systems are considered in [19–25].

Here we elaborate on the model of (zero temperature) attenuators and amplifiers with memory effects that was introduced in Refs. [21,22] where, in the case of a quantum limited attenuator, the capacity was explicitly determined. In this work we generalize this model to thermal attenuators and thermal amplifiers and we derive the corresponding classical capacities, extending the previous results obtained in the memoryless scenario [10]. We have also considered the case of the additive noise channel, viewed as a particular limit of an attenuator with large transmissivity and large thermal noise. This limit is essentially equivalent to the model considered in [24,26], and we have shown that the only effect of the memory is a redistribution of the added noise. An interesting fact which emerges from our analysis is the presence of a critical environmental temperature which strongly affects the distribution of the input energy among the various modes of the model. In particular for temperatures larger than the critical one, only the modes which have a sufficiently high effective transmissivity are allowed to contribute to the signaling process, the remaining one being forced to carry no energy nor information.

Given a quantum channel the associated unitary dilation is not unique and one can imagine different models for

memory effects. Nonetheless our paradigm is expected to cover many real devices such as optical fibers [27,28], microwave systems [29], THz lasers [30], free space communication [31], etc. All physical implementations are known to exhibit time delay and memory effects whenever used at sufficiently high repetition rates. Moreover, especially in microwave and electrical channels, thermal noise is not negligible and will affect the classical capacity. In general, our analysis applies to any physical realization of quantum channels in which memory effects and thermal noise are simultaneously present.

We begin in Sec. II by recalling some basic facts about the memory channel model of Refs. [6,7]. In particular we describe its normal mode decomposition which allows one to express the associated mapping as a tensor product of not necessarily identical single-mode transformations. In Sec. III instead we compute the classical capacity of the setup and discuss some special cases, while in Sec. IV we analyze how the distribution of the input energy among the various modes is affected by the presence of a thermal environment. Conclusions and perspectives are provided in Sec. V.

II. GAUSSIAN MEMORY CHANNELS

In this section we review the model of *Gaussian memory channels* introduced in Refs. [21,22]. We closely follow their analysis showing that this memory channel can be reduced to a collection of memoryless channels by some appropriate encoding and decoding unitary operations.

A. Quantum attenuators and amplifiers

The building blocks of our analysis are single-mode quantum attenuators and amplifiers [6,7]. Let us consider a continuous variable bosonic system [5] described by the creation and annihilation operators a and a^\dagger and another mode described by a^E and $a^{E\dagger}$ associated to the environment. We focus on two important Gaussian unitaries,

$$U_\kappa = e^{\arctan \sqrt{(1-\kappa)/\kappa}(a a^{E\dagger} - a^\dagger a^E)} \quad \text{for } \kappa \in [0, 1], \quad (4a)$$

$$U_\kappa = e^{\arctanh \sqrt{(\kappa-1)/\kappa}(a^\dagger a^{E\dagger} - a a^E)} \quad \text{for } \kappa > 1, \quad (4b)$$

corresponding to the beam splitter and two-mode squeezing operations, respectively. Their action on the annihilation operator is

$$U_\kappa^\dagger a U_\kappa = \sqrt{\kappa} a - \sqrt{1-\kappa} a^E \quad \text{for } \kappa \in [0, 1], \quad (5a)$$

$$U_\kappa^\dagger a U_\kappa = \sqrt{\kappa} a + \sqrt{\kappa-1} a^{E\dagger} \quad \text{for } \kappa > 1. \quad (5b)$$

If the environment is in a Gaussian thermal state $\rho_E = e^{-\beta \hbar \omega a^{E\dagger} a^E} / \text{Tr}[e^{-\beta \hbar \omega a^{E\dagger} a^E}]$ with mean photon number $N = \text{Tr}[a^{E\dagger} a^E \rho] = (e^{\beta \hbar \omega} - 1)^{-1}$, applying the unitaries (5a) and (5b) and tracing out the environment, we get

$$\mathcal{E}_\kappa(\rho) = \text{Tr}_E[U_\kappa(\rho \otimes \rho_E)U_\kappa^\dagger]. \quad (6)$$

This generates two different phase-insensitive channels depending on whether κ is less or larger than 1. For $\kappa \in [0, 1]$ the channel corresponds to a thermal attenuator, while for $\kappa > 1$ the channel is a thermal amplifier. In both cases the classical capacity has been recently determined in [10]. Under the input energy constraint $\text{Tr}[a^\dagger a \rho] \leq E$, the capacities of the attenuator and of the amplifier are obtainable via a Gaussian

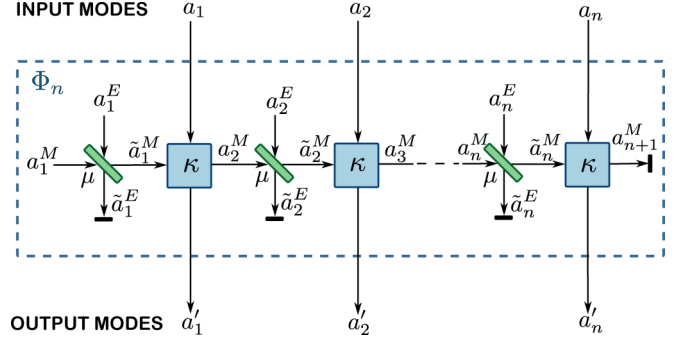


FIG. 1. (Color online) Schematic description of a Gaussian memory channel Φ_n which is iterated n times. The application of the memory channel to n successive input modes a_1, \dots, a_n is described by n phase-insensitive channels \mathcal{E}_κ (thermal attenuators or amplifiers) where each of them is coupled to a Gaussian thermal environment and to a memory mode. The initial memory mode a_1^M travels horizontally and correlates the output signals with the previous input signals. A beam splitter of transmissivity μ is used to tune the memory effect of the channel. For $\mu = 1$ the memory mode is perfectly preserved while for $\mu = 0$ the channel becomes memoryless. A reasonable choice for the initial state of the memory mode is a Gaussian thermal state in equilibrium with the environment, i.e., we make the identification $a_1^M = a_0^E$. The final state of the memory is assumed to be inaccessible and is traced out.

encoding and are given by [10] (in nats for channel use):

$$C_{\kappa \in [0, 1]} = g[\kappa E + (1 - \kappa)N] - g[(1 - \kappa)N], \quad (7a)$$

$$C_{\kappa > 1} = g[\kappa E + (\kappa - 1)(N + 1)] - g[(\kappa - 1)(N + 1)], \quad (7b)$$

where $g(x) = (x + 1) \ln(x + 1) - x \ln(x)$.

B. Gaussian memory channels

In order to include memory effects we follow the model introduced in [21,22] and schematically shown in Fig. 1. In addition to the degrees of freedom of the system and of the thermal environment we introduce a “memory” described by the bosonic operators a^M and $a^{M\dagger}$. The channel acts in the following way: As a first step the memory is mixed with the environment via a beam splitter of transmissivity μ ,

$$\tilde{a}^M = \sqrt{\mu} a^M + \sqrt{1 - \mu} a^E. \quad (8)$$

The outcome state is used as an effective environment for the quantum attenuator or alternatively the quantum amplifier. More precisely, the second step consists in applying the unitary (5a) or (5b) to the product state of the system and of the effective environment,

$$a' = \sqrt{\kappa} a - \sqrt{1 - \kappa} \tilde{a}^M, \quad \kappa \in [0, 1], \quad (9a)$$

$$a' = \sqrt{\kappa} a + \sqrt{\kappa - 1} \tilde{a}^{M\dagger}, \quad \kappa > 1. \quad (9b)$$

The second port of the attenuator or amplifier is given by the corresponding complementary channel,

$$a^{M'} = \sqrt{\kappa} \tilde{a}^M + \sqrt{1 - \kappa} a, \quad \kappa \in [0, 1], \quad (10a)$$

$$a^{M'} = \sqrt{\kappa} \tilde{a}^M + \sqrt{\kappa - 1} \tilde{a}^\dagger, \quad \kappa > 1. \quad (10b)$$

The complementary mode described by the annihilation operator $a^{M'}$ contains a fraction of the amplitudes of the input state, and represents the updated state of the memory, i.e., in the next use of the channel, the mode $a^{M'}$ will play the role of the previous memory operator a^M . Once the initial states of the memory and of the environment are specified, the action of the channel after j uses is completely determined and can be computed recursively. The explicit formula for the j th output mode can be found in [22] and is not repeated here. What is important is just the structure of the equations

$$a'_j = \sum_{h=1}^{j-1} A_{jh} a_h - \sum_{h=0}^j E_{jh} a_h^E, \quad \kappa \in [0, 1], \quad (11a)$$

$$a'_j = \sum_{h=1}^{j-1} A_{jh} a_h + \sum_{h=0}^j E_{jh} a_h^{E\dagger}, \quad \kappa > 1, \quad (11b)$$

where A and E are real matrices and the initial state of the memory has been identified with an additional mode of the environment $a^M = a_0^E$. Moreover the following identities hold:

$$\sum_{k=1}^n (A_{ik} A_{jk} + E_{ik} E_{jk}) = \delta_{ij}, \quad \kappa \in [0, 1], \quad (12a)$$

$$\sum_{k=1}^n (A_{ik} A_{jk} - E_{ik} E_{jk}) = \delta_{ij}, \quad \kappa > 1. \quad (12b)$$

This implies that there exist some orthogonal matrices O, O', O'' realizing the following singular value decompositions [22]:

$$A_{jh} = \sum_{j'=1}^n O_{jj'} \sqrt{\eta_{j'}^{(n)}} O'_{j'h}, \quad (13a)$$

$$E_{jh} = \sum_{j'=1}^n O_{jj'} \sqrt{|\eta_{j'}^{(n)} - 1|} O''_{j'h}, \quad (13b)$$

where $\eta_j^{(n)}$ are positive real numbers and the matrix O is the same in both decompositions. In terms of the following set of collective modes:

$$a'_j := \sum_{j'=1}^n O_{j'j} a'_{j'}, \quad (14a)$$

$$a_j := \sum_{j'} O'_{jj'} a_{j'}, \quad (14b)$$

$$a_j^E := \sum_{j'} O''_{jj'} a_{j'}^E, \quad (14c)$$

the memory channel is diagonalized into n independent channels,

$$a'_j = \sqrt{\eta_j^{(n)}} a_j - \sqrt{1 - \eta_j^{(n)}} a_j^E, \quad \kappa \in [0, 1], \quad (15a)$$

$$a'_j = \sqrt{\eta_j^{(n)}} a_j + \sqrt{\eta_j^{(n)} - 1} a_j^{E\dagger}, \quad \kappa > 1. \quad (15b)$$

In particular, if we focus on the physically relevant case in which all the modes of the environment (and the initial memory

mode) are in the same thermal state with a given mean photon number N , the modes $\{a_j^E\}$ remain in factorized thermal states and one can conclude that the memory channel applied n times is unitarily equivalent to n independent memoryless attenuators or amplifiers,

$$\Phi_n = \mathcal{E}_{\eta_1^{(n)}}^N \otimes \mathcal{E}_{\eta_2^{(n)}}^N \cdots \otimes \mathcal{E}_{\eta_n^{(n)}}^N. \quad (16)$$

An important feature of the canonical transformation (14b) is that annihilation operators a_j are not mixed with creation operators a_j^\dagger . This means that the operation is passive, i.e., it does not change the total energy of the input modes and so the capacity with constrained input energy is the same for the diagonalized channel and the original one.

C. Limit of infinite iterations

In order to compute the capacity we need to take the limit infinite iterations of the memory channel. In virtue of the previous factorization into independent channels, the capacity will depend only on the asymptotic distribution of the gain parameters $\eta_j^{(n)}$ appearing in (16), in the limit of $n \rightarrow \infty$. The set of gain parameters $\eta_j^{(n)}$ can be computed as the eigenvalues of the matrix

$$M^{(n)} := AA^\dagger. \quad (17)$$

The entries of the matrix M can be computed from the explicit values of A [22], obtaining

$$M_{jj'}^{(n)} = \delta_{jj'} + (\kappa_{jj'} - 1) \sqrt{\mu\kappa}^{|j-j'|}, \quad (18)$$

where

$$\kappa_{jj'} := \kappa + \mu(\kappa - 1)^2 \sum_{h=0}^{\min\{j,j'\}-2} (\mu\kappa)^h. \quad (19)$$

The asymptotic behavior of the eigenvalues is different according to whether the combination $\mu\kappa$ is greater or lower than 1. Below threshold, i.e., for $\mu\kappa < 1$ the sequence of matrices $M^{(n)}$ is *asymptotically equivalent* [32] to the (infinite) Toeplitz matrix $M^{(\infty)}$, given by

$$M_{jj'}^{(\infty)} := M_{j-j'}^{(\infty)} = \delta_{jj'} - \frac{(1-\mu)(1-\kappa)}{1-\kappa\mu} \sqrt{\mu\kappa}^{|j-j'|}. \quad (20)$$

We can now exploit the full power of the Toeplitz matrices theory (see Ref. [32] for more details): The Szegő theorem [32] states that, for any smooth function F , we have

$$\lim_{n \rightarrow \infty} \frac{1}{n} \sum_{j=1}^n F[\eta_j^{(n)}] = \int_0^{2\pi} \frac{dz}{2\pi} F[\eta(z)], \quad (21)$$

where the function $\eta(z)$ is the Fourier transform of the elements of the matrix $M^{(\infty)}$, i.e.,

$$\eta(z) = \sum_{j=-\infty}^{\infty} M_j^{(\infty)} e^{izj/2} = \frac{\kappa + \mu - 2\sqrt{\kappa\mu} \cos \frac{z}{2}}{1 + \kappa\mu - 2\sqrt{\kappa\mu} \cos \frac{z}{2}}, \quad (22)$$

with $z \in [0, 2\pi]$ (see Figs. 2 and 3).

Above threshold, i.e., for $\mu\kappa > 1$, the sequence of matrices does not converge. Nonetheless, the divergence can be ascribed

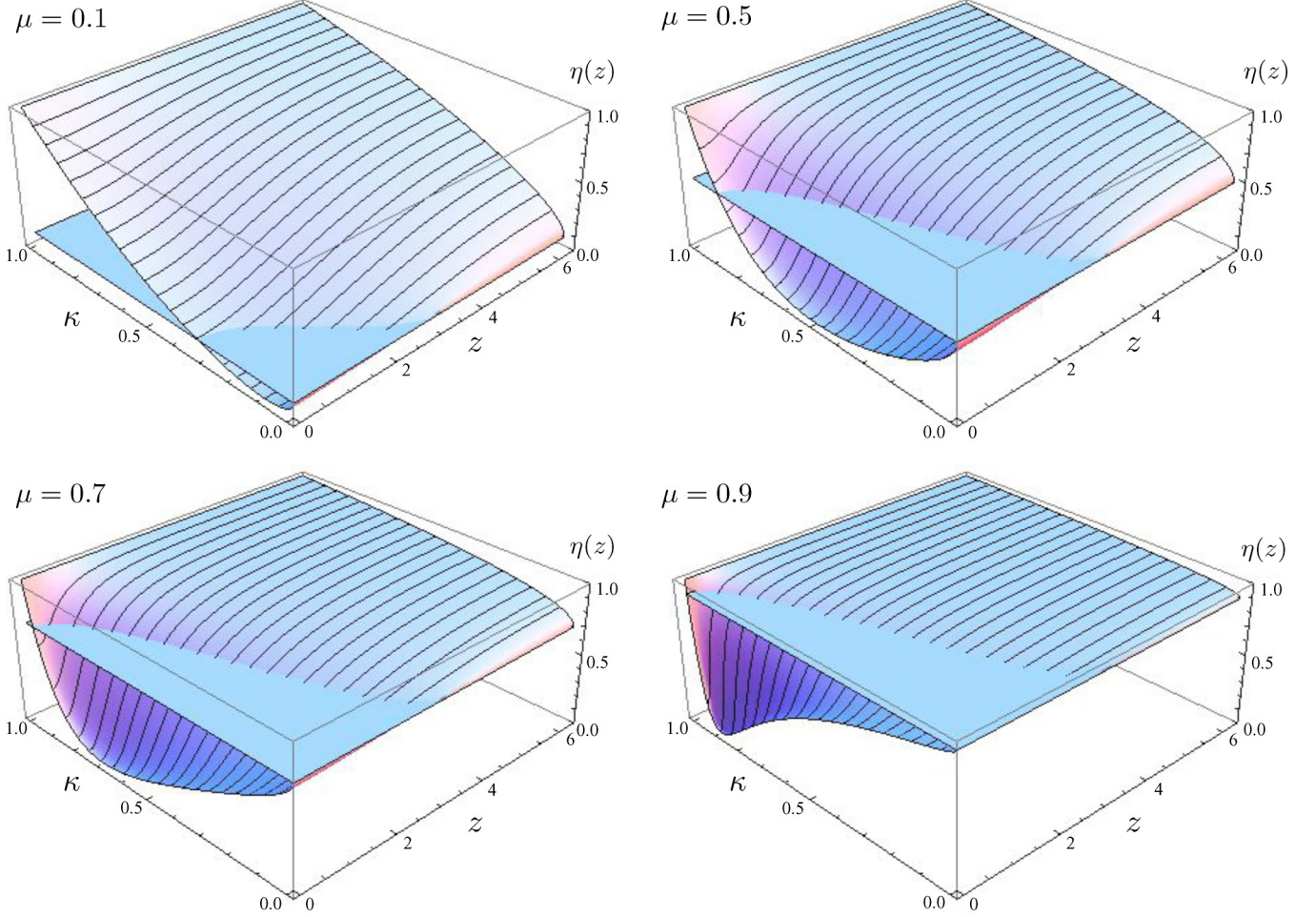


FIG. 2. (Color online) Asymptotic spectrum $\eta(z)$ of Eq. (22) for the case where \mathcal{E}_κ of Fig. 1 represents an attenuator channel (i.e., $\kappa \in [0, 1]$). In this case the system is operated below the threshold limit $\mu\kappa \leq 1$ (no divergency in the spectrum occurs) and the values of $\eta(z)$ are always bounded below 1 (i.e., the channels $\mathcal{E}_{\eta_j}^N$ entering the decomposition (16) are attenuators). In each plot the plane represents the value of μ . Notice that for $\kappa = 0$ one has $\eta(z) = \mu$, while for $\kappa = 1$, $\eta(z) = 1$ independently from η .

to a single diverging eigenvalue, and it is possible to rewrite Eq. (18) as the sum of two terms:

$$M^{(n)} = c^{(n)} P^{(n)} + \Delta M^{(n)}, \quad (23)$$

where the $P^{(n)}$ are rank-one projectors, $c^{(n)}$ is a diverging sequence of positive real numbers, and $\Delta M^{(n)}$ is a sequence of matrices which asymptotically converges towards the (infinite) Toeplitz matrix $\Delta M^{(\infty)}$, given by

$$\Delta M_{jj'}^{(\infty)} = \delta_{jj'} + \frac{(1-\mu)(\kappa-1)}{\mu\kappa-1} \frac{1}{\sqrt{\mu\kappa}^{|j-j'|}}. \quad (24)$$

(See the appendix of [22] for the expressions of $P^{(n)}$ and $\Delta M^{(n)}$). It is possible to prove that for $n \rightarrow \infty$, the matrices $P^{(n)}$ and $\Delta M^{(n)}$ commute, and we can conclude that, as promised, the spectrum of the matrix (18) is asymptotically composed of only one diverging eigenvalue [corresponding to the diverging sequence $c^{(n)}$] and of the asymptotic spectrum of the infinite Toeplitz matrix (24). As for the below threshold case, the latter is given by the Fourier transform of the matrix

elements, where the Fourier transform $\eta(z)$ is given by Eq. (22) analytically continued to the region $\mu\kappa > 1$.

Finally it remains to consider the case $\mu\kappa = 1$. At this threshold, the matrix $M^{(n)}$ can be expressed as

$$M_{jj'}^{(n)} = \delta_{jj'} + (1-\mu) + \frac{(1-\mu)^2}{\mu} \min\{j, j'\}. \quad (25)$$

In this case it appears not feasible to extract the asymptotic spectrum. From a practical point of view, however, this is not a real problem since any real physical channel will always fall into one of the two classes characterized by $\mu\kappa > 1$ or $\mu\kappa < 1$, respectively.

It is important to stress that for any $\mu \in [0, 1]$, in the thermal attenuator case ($\kappa \in [0, 1]$) all the channels in the asymptotic diagonal decomposition (16) are also thermal attenuators, i.e., $\eta(z) \in [0, 1]$ for any $z \in [0, 2\pi]$. The same happens in the amplifier case, i.e., if $\kappa > 1$ also $\eta(z) > 1$ for any $z \in [0, 2\pi]$.

III. CAPACITIES

In this section we will compute the capacity of the memory channel model of the previous section, with the environment

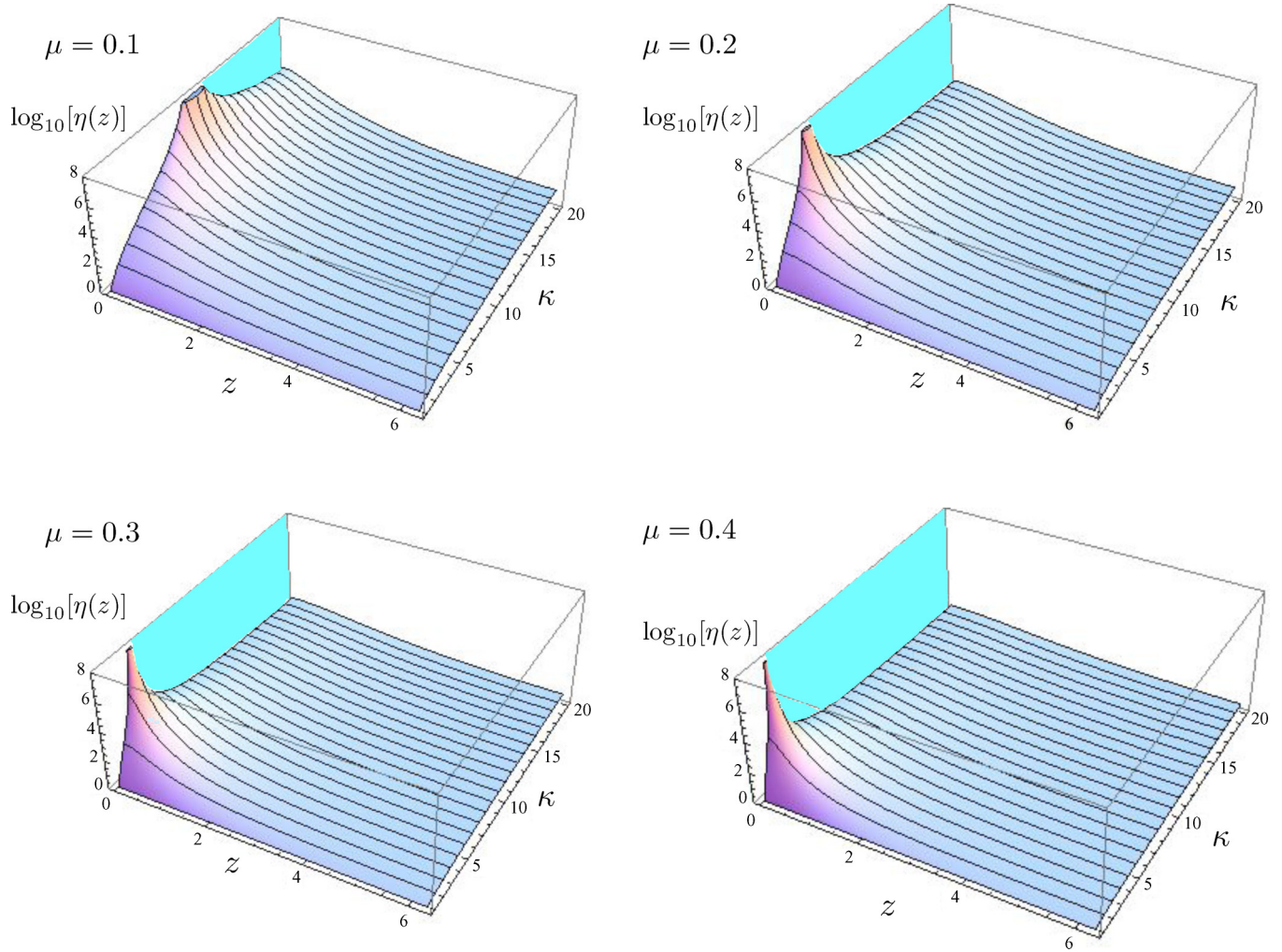


FIG. 3. (Color online) Logarithm of the asymptotic spectrum $\eta(z)$ of Eq. (22) for the case where \mathcal{E}_κ of Fig. 1 represents an amplifier channel (i.e., $\kappa \geq 1$). In this case the values of $\eta(z)$ are always larger than 1 meaning that the channels $\mathcal{E}_{\eta_j^{(n)}}^N$ entering the decomposition (16) describe amplifiers. Above threshold (i.e., $\mu\kappa \geq 1$) the system acquires also a divergent, singular eigenvalue represented in the picture by the cyan vertical region.

in a thermal multimode state with fixed temperature and associated mean photon number per mode N .

Let Φ_P be the mapping describing the input-output relations of the first P -channel uses of the model depicted in Fig. 1. Since any input influences all the following outputs, its classical capacity cannot be directly computed as in Eq. (1). Still, thanks to the fact that Φ_P can be expressed as a tensor product of $P \gg 1$ independent maps of effective transmissivities $\eta_j^{(P)}$ [see Eq. (16)], a close formula for C can be derived. The fundamental observation here is that, even though in general the $\eta_j^{(P)}$ will differ from each other, for large enough P one can organize them into subgroups each containing a number of elements of order P , and characterized by an almost identical value of the transmissivity distributed according to the continuous function $\eta(z)$ of Eq. (22). Consider next the channel Φ_{2P} . Its effective transmissivities are different, but they are taken from almost the same distribution, therefore we can write

$$\Phi_{2P} \simeq \Phi_P \otimes \Phi_P. \quad (26)$$

Iterating, we get

$$\Phi_{\ell P} \simeq \Phi_P^{\otimes \ell}, \quad (27)$$

and we have managed to express Φ_n for $n \rightarrow \infty$ as the limit of infinite uses of a fixed memoryless channel.

Let us formalize this procedure: We fix $P \gg 1$, and take $n = \ell P$. We label the eigenvalues $\eta_j^{(n)}$ in increasing order ($\eta_j^{(n)} \leq \eta_{j'}^{(n)}$ if $j < j'$), and divide them into P groups, the p th one being made by $\{\eta_j^{(n)} | (p-1)\ell < j \leq p\ell\}$. Let $\underline{\eta}_p^{(P)}$ and $\bar{\eta}_p^{(P)}$ be, respectively, the infimum and the supremum of the p th group over all ℓ :

$$\underline{\eta}_p^{(P)} = \inf_{\ell} \inf_{(p-1)\ell < j \leq p\ell} \eta_j^{(\ell P)}, \quad (28a)$$

$$\bar{\eta}_p^{(P)} = \sup_{\ell} \sup_{(p-1)\ell < j \leq p\ell} \eta_j^{(\ell P)}. \quad (28b)$$

Now, the two collections of transmissivities $\underline{\eta}_p^{(P)}$ and $\bar{\eta}_p^{(P)}$ identify two memoryless P -mode Gaussian channels. Let $\phi(\eta, N)$ be the Gaussian attenuator or amplifier with

transmissivity $\eta \geq 0$, mixing the input with a thermal state with mean photon number N . Remembering that $\phi(\eta, N)\phi(\eta', N) = \phi(\eta\eta', N)$ and that the capacity decreases under composition of channels, if we replace each transmissivity with the supremum or the infimum of its group, the capacity will increase or decrease, respectively. Each group has exactly ℓ eigenvalues, so the n uses of the single-mode memory channel can be compared to ℓ uses of these two P -mode channels, and letting $\ell \rightarrow \infty$ we can bound the capacity with

$$\underline{C}^{(P)} \leq C \leq \overline{C}^{(P)}, \quad (29)$$

where $\underline{C}^{(P)}$ and $\overline{C}^{(P)}$ are precisely the capacities of these P -mode channels with transmissivities $\{\underline{\eta}_p^{(P)}\}, \{\overline{\eta}_p^{(P)}\}$. As customary, to keep them finite we impose a constraint on the input mean energy:

$$\frac{1}{n} \sum_{j=1}^n \text{Tr}[\rho^{(n)} a_j^\dagger a_j] \leq E, \quad (30)$$

where n is the number of uses of the channel and $\rho^{(n)}$ is the joint input density matrix. As already stressed, this constraint looks identical if expressed in terms of the collective modes (14b), since they are related to the original ones by an orthogonal matrix.

A. Thermal attenuator

Let us first consider the case of the attenuating thermal memory channel, i.e., $\kappa \leq 1$. It has recently been proven [8] that the χ capacity of successive uses of Gaussian phase-insensitive channels is additive also if they are different:

$$\chi(\Phi_1 \otimes \cdots \otimes \Phi_n) = \chi(\Phi_1) + \cdots + \chi(\Phi_n). \quad (31)$$

Then the capacity of our two P -mode channels can be simply obtained by summing (7a) over all modes, yielding the bounds

$$\underline{C}^{(P)} = \frac{1}{P} \sum_{p=1}^P (g[\underline{\eta}_p^{(P)} \underline{N}_p + (1 - \underline{\eta}_p^{(P)}) N_T] + g[(1 - \underline{\eta}_p^{(P)}) N_T]), \quad (32a)$$

$$\overline{C}^{(P)} = \frac{1}{P} \sum_{p=1}^P (g[\overline{\eta}_p^{(P)} \overline{N}_p + (1 - \overline{\eta}_p^{(P)}) N_T] + g[(1 - \overline{\eta}_p^{(P)}) N_T]), \quad (32b)$$

where

$$g(x) = (x + 1) \ln(x + 1) - x \ln x, \quad (33)$$

and the parameters $\underline{N}_p, \overline{N}_p$ describe the optimal distribution of the mean photon number of the modes and must satisfy the constraints

$$\underline{N}_p, \overline{N}_p \geq 0, \quad (34a)$$

$$\frac{1}{P} \sum_{p=1}^P \underline{N}_p = \frac{1}{P} \sum_{p=1}^P \overline{N}_p = E. \quad (34b)$$

If the positivity constraint (34a) were not there, these optimal values could be computed with the Lagrange multiplier

method, yielding

$$\underline{N}_p = \frac{1}{\underline{\eta}_p^{(P)}} \left(\frac{1}{e^{\lambda/\underline{\eta}_p^{(P)}} - 1} - (1 - \underline{\eta}_p^{(P)}) N \right), \quad (35)$$

and the analog for \overline{N}_p . Taking the limit $P \rightarrow \infty$ and applying (21), the two bounds converge to the same quantity and we get

$$C = \int_0^{2\pi} \frac{dz}{2\pi} (g(\eta(z)N(z) + [1 - \eta(z)]N) + g([1 - \eta(z)]N)), \quad \kappa \in [0, 1]. \quad (36)$$

In the zero temperature case $N = 0$ the expression (35) is positive definite. As N grows, (35) is no longer guaranteed to be positive, and we have to impose this constraint by hand. Then, above a certain critical temperature the optimal energy distribution $N(z)$ will vanish for $0 \leq z \leq z_0$. Physically, this means that it is convenient to concentrate all the energy on a fraction $\frac{2\pi - z_0}{2\pi}$ of all the beam splitters. We will show in Sec. IV that to determine the optimal energy distribution we can still use the Lagrange multipliers, with the only caveat that $N(z)$ is given now by the positive part of what we would have got without the energy constraint:

$$N(z) = \frac{1}{\eta(z)} \left(\frac{1}{e^{\lambda/\eta(z)} - 1} - [1 - \eta(z)]N \right)^+, \quad (37)$$

where $f^+(z) = [f(z) + |f(z)|]/2$ is the positive part of f . The energy constraint reads as expected:

$$\int_0^{2\pi} \frac{dz}{2\pi} N(z) = E. \quad (38)$$

We notice that the function η is symmetric in μ and κ , i.e.,

$$\eta(\mu, \kappa, z) = \eta(\mu' = \kappa, \kappa' = \mu, z). \quad (39)$$

Since μ and κ appear in the computation of the capacity only through η , the channel with parameters (μ', κ') has the same capacity of the original one, i.e., we can exchange the memory with the transmissivity. Then, varying the memory with fixed transmissivity has the same effect on the capacity as varying the transmissivity for fixed memory. In Fig. 4 we report the capacity of the channel as a function of the temperature.

B. Thermal amplifier

The minimum output entropy conjecture lets us compute the capacity also in the amplifier case $\kappa > 1$. Now, all the transmissivities are greater than 1, so the capacity decreases as they increase and the two bounds (32) are inverted:

$$\overline{C}^{(P)} = \frac{1}{P} \sum_{p=1}^P (g[\underline{\eta}_p^{(P)} \underline{N}_p + (\underline{\eta}_p^{(P)} - 1)(N + 1)] + g[(\underline{\eta}_p^{(P)} - 1)(N + 1)]), \quad (40a)$$

$$\underline{C}^{(P)} = \frac{1}{P} \sum_{p=1}^P (g[\overline{\eta}_p^{(P)} \overline{N}_p + (\overline{\eta}_p^{(P)} - 1)(N + 1)] + g[(\overline{\eta}_p^{(P)} - 1)(N + 1)]). \quad (40b)$$

As in the thermal attenuator case, we take the limit $P \rightarrow \infty$. Above the threshold ($\mu\kappa > 1$) one of the eigenvalues is

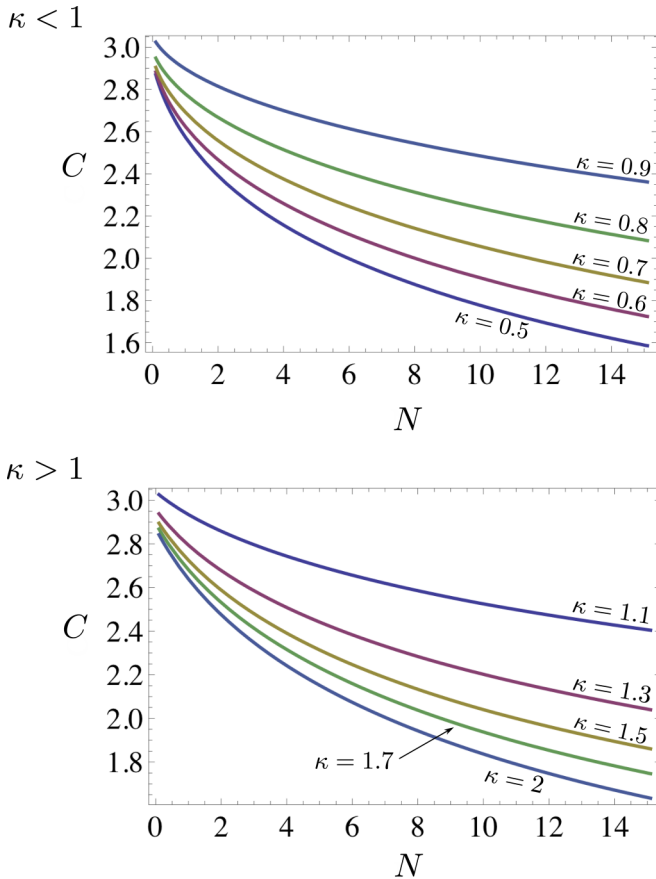


FIG. 4. (Color online) Capacity (in nats/channel use) as a function of the thermal photon number N for $\mu = 0.8$ and mean input energy $E = 8$ for various values of the transmissivity κ . In particular the upper panel refers to the case where the map \mathcal{E}_κ of Fig. 1 is an attenuator (i.e., $\kappa \in [0, 1]$), while the lower panel refers to the case where \mathcal{E}_κ is an amplifier ($\kappa \geq 1$). As expected, the capacity is degraded by the temperature and enhanced if the transmissivity is close to unity.

diverging but, being only one, it does not contribute in the limit, so the capacity is still fully determined by the infinite Toeplitz matrix $\Delta M^{(\infty)}$ yielding

$$C = \int_0^{2\pi} \frac{dz}{2\pi} (g(\eta(z)N(z) + [\eta(z) - 1](N + 1)) + g([\eta(z) - 1](N + 1))), \quad (41)$$

where as before $N(z)$ is determined by the Lagrange multiplier method, with the caveat of taking the positive part of the resulting function

$$N(z) = \frac{1}{\eta(z)} \left(\frac{1}{e^{\frac{\lambda}{\eta(z)}} - 1} - [\eta(z) - 1](N + 1) \right)^+, \quad (42)$$

and with the same constraint on the mean energy

$$\int_0^{2\pi} \frac{dz}{2\pi} N(z) = E. \quad (43)$$

We notice that in (42) the positive part is at least in principle necessary also in the case of zero temperature.

Also the amplifier enjoys a sort of duality between κ and μ : The function $\eta(\mu, \kappa, z)$ satisfies

$$\eta(\mu, \kappa, z) = \eta\left(\mu' = \frac{1}{\kappa}, \kappa' = \frac{1}{\mu}, z\right). \quad (44)$$

Noticing that $\kappa'\mu' = \frac{1}{\kappa\mu}$, this relation associates to any channel identified by (μ, κ) above threshold ($\mu\kappa > 1$) the new one identified by (μ', κ') , which is below threshold. Then, to investigate the capacity regions as a function of the parameters, it is sufficient to consider only the channels below threshold.

In Fig. 4 we report the capacity of the thermal memory channel as a function of the thermal photon number N . As for the thermal attenuator, the capacity is degraded by the temperature and enhanced by the memory.

C. Optimal encoding and decoding

We have seen how the optimal encoding is a coherent-state one with Gaussian weights in the normal mode decomposition $\{a_j\}$ introduced in Eq. (14b) in which the channel is diagonal. They are related to the input modes $\{a_j\}$ by a passive orthogonal transformation, and since such transformations send coherent states to coherent states, the latter are also not entangled. However, since the optimal coding requires a nonuniform energy distribution among the $\{a_j\}$, the modes $\{a_j\}$ will be classically correlated. Then this optimal coding can be achieved by independent uses of the channel, but the probabilities of choosing a particular coherent state will be correlated among the various inputs.

Since also in the case of multiple uses of a fixed memoryless channel the optimal decoding requires measures entangled among the various outputs [2], in our case the preprocessing with an orthogonal passive transformation to convert the physical basis into the diagonal one does not add further complications to the procedure.

Above threshold ($\mu\kappa > 1$), the diverging eigenvalue signals the presence of an input mode that gets amplified by a factor which increases indefinitely with the number of channel uses. Then, even if such mode is left in the vacuum, the corresponding output mode will have a very high energy, and could in principle lead the beam splitter used in the decoding procedure to a nonlinear regime. The experimentally achievable capacity could then be lower than the theoretical bound, depending on the stability of the decoding device when dealing with high energy inputs.

D. Trivial cases

There are some particular values of the parameters for which the capacity can be computed analytically.

(1) $\kappa = 1$ or $\mu = 1$. This case corresponds to the identity channel ($\kappa = 1$) or to the perfect memory channel ($\mu = 1$). In both cases, $\eta(z) = 1$ and the capacity is that of the identity channel with mean energy E :

$$C = g(E). \quad (45)$$

An intuitive explanation of the result for the perfect memory channel can be given: Since $\mu = 1$, the first n output modes $\{a'_i\}$ are a linear combination only of the first n input modes $\{a_i\}$ and the first memory mode a_1^M , and the environment modes

$\{a_i^E\}$ do not play any role. Now we can imagine that in the large n limit the mode a_i^M is no more relevant, and the channel behaves almost as if the output modes were an invertible linear combination of the input ones. This combination can be inverted in the decoding, recovering (almost) the identity channel.

(2) $\kappa \rightarrow \infty$. This is the case of infinite amplification. Here $\eta(z) = \frac{1}{\mu}$, and the capacity is that of the amplifier with amplification factor $\frac{1}{\mu}$:

$$C = g\left(\frac{E}{\mu} + \frac{1-\mu}{\mu}(N+1)\right) - g\left(\frac{1-\mu}{\mu}(N+1)\right). \quad (46)$$

(3) $\kappa = 0$. This is the case of infinite attenuation, in which all the signal is provided by the memory. Here the n th input mode a_n does not influence at all the n th output a'_n , but it directly mixes with the $(n+1)$ th environmental mode a_{n+1}^E through the beam splitter with transmissivity μ to give the $(n+1)$ th output a'_{n+1} . Then the only memory effect is a translation of the inputs, and the channel behaves as a thermal attenuator with transmissivity μ . Indeed, as shown in Fig. 2, here $\eta(z) = \mu$, and the capacity matches the attenuator one [10]:

$$C = g[\mu E + (1-\mu)N] - g[(1-\mu)N]. \quad (47)$$

(4) $\mu = 0$. This is the memoryless case, and the capacity is that of the thermal attenuator or amplifier with transmissivity κ :

$$C = g[\kappa E + (1-\kappa)N] - g[(1-\kappa)N], \quad (48a)$$

$$C = g[\kappa E + (\kappa-1)(N+1)] - g[(\kappa-1)(N+1)]. \quad (48b)$$

E. Additive noise channel

The one-mode additive noise channel adds to the covariance matrix σ of the input state a multiple of the identity:

$$\sigma \mapsto \sigma + N_C \mathbb{1}. \quad (49)$$

A beam splitter of transmissivity η , mixing the input with a thermal state with mean photon number N , performs instead a convex combination of the corresponding covariance matrices:

$$\sigma \mapsto \eta\sigma + (1-\eta)\left(N + \frac{1}{2}\right)\mathbb{1}. \quad (50)$$

The additive noise channel can now be recovered in the limit $\eta \rightarrow 1^-$ with the second addend of (50) kept fixed, i.e., with

$$(1-\eta)\left(N + \frac{1}{2}\right) = N_C, \quad \eta \rightarrow 1^-, \quad N \rightarrow \infty. \quad (51)$$

It is then natural to consider what happens to our model for the memory channel in the limit $N \rightarrow \infty$, $\kappa \rightarrow 1^-$ with fixed $(1-\kappa)(N + \frac{1}{2}) = N_C$. We start from the expression (11a) which expresses the output modes in terms of the input and the (thermal) environment. From the expressions for the matrices A and E in [22] it is easy to show that, since they do not depend on N , their limits for $\kappa \rightarrow 1$ are $A \rightarrow \mathbb{1}$ and $E \rightarrow 0$, respectively. Physically, this happens because for $\kappa = 1$ the channel is the identity and the output is equal to the input. We will now compute the expectation values of all the operators quadratic in the output modes, i.e., the output covariance matrix. We remember that, since the input and the environment

are in a completely factorized state,

$$\langle a_i a_j^E \rangle = \langle a_i^\dagger a_j^E \rangle = \langle a_i^E a_j^E \rangle = 0, \quad (52a)$$

$$\langle a_i^E a_j^E \rangle = N \delta_{ij}. \quad (52b)$$

We have then

$$\langle a'_i a'_j \rangle = \langle a_i a_j \rangle, \quad (53a)$$

$$\langle a_i^\dagger a'_j \rangle = \langle a_i^\dagger a_j \rangle + \lim_{N \rightarrow \infty} N \sum_k E_{ik} E_{jk}, \quad (53b)$$

where the limit is nontrivial since the matrix E depends on κ , which changes with N . Recalling (12a),

$$AA^T + EE^T = \mathbb{1}, \quad (54)$$

and from the expression for $AA^T = AA^\dagger$ in [22] it is easy to prove that

$$\lim_{N \rightarrow \infty} N \sum_k E_{ik} E_{jk} = N_C \mu^{|i-j|/2}, \quad (55)$$

so

$$\langle a_i^\dagger a'_j \rangle = \langle a_i^\dagger a_j \rangle + N_C \mu^{|i-j|/2}. \quad (56)$$

If we look only at a single output mode a'_i , throwing away all the others, (56) becomes

$$\langle a_i^\dagger a'_i \rangle = \langle a_i^\dagger a_i \rangle + N_C, \quad (57)$$

i.e., the reduced channel exactly adds classical noise N_C . However, for nonzero memory ($\mu > 0$), $N_C \mu^{|i-j|/2}$ is nonzero also for $i \neq j$: The added noise is correlated among the various outputs, and the resulting channel is not simply the product of n independent additive noise ones. We expect this correlation to enhance the capacity: Looking at the limit of our formula (36), we will see that it is effectively so. Let us look at this limit in the normal mode variables. Remembering that the environment associated to the operators a_j^E is still in a factorized thermal state with temperature N , we have

$$\langle a'_i a'_j \rangle = \langle a_i a_j \rangle, \quad (58a)$$

$$\langle a_i^\dagger a'_j \rangle = \langle a_i^\dagger a_j \rangle + \delta_{ij} \lim_{N \rightarrow \infty} N(1 - \eta_i^{(n)}), \quad (58b)$$

and since

$$\lim_{N \rightarrow \infty} [1 - \eta(z)]N = \frac{N_C(1-\mu)}{1 + \mu - 2\sqrt{\mu} \cos \frac{z}{2}}, \quad (59)$$

in the limit of infinite channel uses we get a factorized additive noise channel, but with the added noise depending on the mode and distributed according to (59). This model for an additive noise channel with memory coincides with the one considered in [24,26], derived starting from correlated translations with Gaussian weights.

First, notice that $\eta(z)$ does not depend on N , and $\lim_{\kappa \rightarrow 1} \eta(z) = 1$. Let us compute the limit of the expression for $N(z)$ (37):

$$N(z) = \left(\frac{1}{e^\lambda - 1} - \lim_{N \rightarrow \infty} [1 - \eta(z)]N \right)^+. \quad (60)$$

From the expression for $\eta(z)$ (22) we can compute the limit so that

$$N(z) = \left(\frac{1}{e^\lambda - 1} - \frac{N_C(1 - \mu)}{1 + \mu - 2\sqrt{\mu} \cos \frac{z}{2}} \right)^+. \quad (61)$$

For simplicity, we consider only the case in which the positive part in (61) is not needed. The mean energy constraint (38) becomes

$$\frac{1}{e^\lambda - 1} = N_C + E, \quad (62)$$

where we have used that

$$\int_0^{2\pi} \frac{1 - \mu}{1 + \mu - 2\sqrt{\mu} \cos \frac{z}{2}} \frac{dz}{2\pi} = 1, \quad (63)$$

and we have for the positivity constraint on $N(z)$

$$E \geq \frac{2N_C\sqrt{\mu}}{1 - \sqrt{\mu}}. \quad (64)$$

Finally, we can compute the capacity taking the limit of (36):

$$C = g(E + N_C) - \int_0^{2\pi} g \left(\frac{N_C(1 - \mu)}{1 + \mu - 2\sqrt{\mu} \cos \frac{z}{2}} \right). \quad (65)$$

Since $g(x)$ is concave, the left-hand side of (65) decreases if we take the integral inside g , so

$$C \geq g(E + N_C) - g(N_C). \quad (66)$$

The right-hand side of (66) is exactly the capacity of the single-mode additive noise channel, i.e., the correlation of the added noise enhances the capacity as expected.

IV. OPTIMAL ENERGY DISTRIBUTION

In this section we will prove that the Lagrange multipliers method with the caveat of taking the positive part in (37) and (42) works also with the positivity constraint (34a), and we will analyze the resulting optimal energy distribution $N(z)$.

A. The proof

The function $\eta(z)$ is increasing for the thermal attenuator ($\kappa < 1$) and decreasing for the amplifier ($\kappa > 1$), i.e., the channel with transmissivity $\eta(z)$ always improves as z increases. For simplicity here we consider only the thermal attenuator case, the amplifier one being completely analogous.

Let $\tilde{N}(z, w)$ be the Lagrange multipliers solution in the interval $w \leq z \leq 2\pi$ which maximizes the capacity

$$C = \int_w^{2\pi} \frac{dz}{2\pi} (g[\eta(z)\tilde{N}(z, w) + [\eta(z) - 1](N + 1)] - g([\eta(z) - 1](N + 1))) \quad (67)$$

with the mean energy constraint

$$\int_w^{2\pi} \frac{dz}{2\pi} \tilde{N}(z, w) dz = E, \quad (68)$$

where the integrals are restricted to $w \leq z \leq 2\pi$ and we do not care about the positivity of $N(z, w)$. Such solution is

given by

$$\tilde{N}(z, w) = \frac{1}{\eta(z)} \left(\frac{1}{e^{\frac{\lambda}{\eta(z)}} - 1} - [1 - \eta(z)]N \right), \quad (69)$$

where the multiplier λ is determined by the constraint (68) [strictly speaking, with $\tilde{N}(z, w)$ we mean the function analytically continued to the whole interval $0 \leq z \leq 2\pi$].

Let $N(z)$ be the optimal positive distribution of the photons. Since it is better to use more energy in the better channels, $N(z)$ must be increasing: if not, we could move a bit of energy from a bad channel to a better one with less energy, and this would increase the capacity. Let $N(z)$ be zero for $0 \leq z < z_0$, and strictly positive for $z_0 < z \leq 2\pi$. In particular $N(z)$ is the optimal solution among all the functions equal to zero for $0 \leq z < z_0$ and strictly positive for $z_0 < z \leq 2\pi$. We consider all the infinitesimal variations $N(z) + \delta N(z)$ satisfying the mean energy constraint and such that $\delta N(z)$ is nonzero only in the interval $z_0 < z \leq 2\pi$. Since $N(z)$ is strictly positive there, $N(z) + \delta N(z)$ is still positive for infinitesimal δN , so it is a legal positive photon distribution. For its optimality $N(z)$ must be a stationary point of the capacity for all such variations, but this means exactly that $N(z)$ is the solution of the Lagrange multipliers method $\tilde{N}(z, z_0)$:

$$N(z) = \tilde{N}(z, z_0)\theta(z - z_0), \quad (70)$$

where $\theta(z)$ is the step function.

We now claim that $\tilde{N}(z_0, z_0)$ must be zero. Let us suppose $\tilde{N}(z_0, z_0) > 0$. Since $\tilde{N}(z, w)$ is continuous in w , we can choose a $w_0 < z_0$ such that $\tilde{N}(z, w_0)$ is strictly positive in the whole interval $w_0 < z \leq 2\pi$. Then, $\tilde{N}(z, w_0)\theta(z - w_0)$ is an admissible solution. From its definition (67), $\tilde{N}(z, w_0)$ achieves the maximum capacity among all the energy distributions vanishing for $0 \leq z < w_0$. Since also $N(z)$ belongs to this set, the two functions must coincide for $z > w_0$, and $\tilde{N}(z, w_0)$ cannot be positive for $w_0 < z < z_0$ as assumed.

For the same argument used with $N(z)$, $\tilde{N}(z, z_0)$ must be increasing within each interval where it is positive, and since it is continuous in z it must be negative for $0 \leq z < z_0$ and positive for $z_0 < z \leq 2\pi$. Then we can finally write as promised $N(z)$ as

$$N(z) = \frac{1}{\eta(z)} \left(\frac{1}{e^{\lambda/\eta(z)} - 1} - [1 - \eta(z)]N \right)^+, \quad z \in [0, 2\pi], \quad (71)$$

where $f^+(z)$ is the positive part of f .

B. Analysis of the optimal distribution

The typical behavior of $N(z)$ in the attenuator case is shown in Fig. 5. It is increasing, as it has to be. We can identify a critical temperature N_{crit} , that for our choice of the parameters ($\kappa = 0.9$, $\mu = 0.8$, $E = 8$) is nearly $N_{\text{crit}} \sim 0.8$. Below this critical value, $N(z)$ approaches a constant positive value for $z \rightarrow 0$, i.e., the optimal configuration exploits all the beam splitters. Above the critical value, $N(z)$ is zero on a finite interval $[0, z_0]$, i.e., the optimal configuration does not use at all a finite fraction $\frac{z_0}{2\pi}$ of the beam splitters, being more convenient to concentrate all the energy on the other ones.

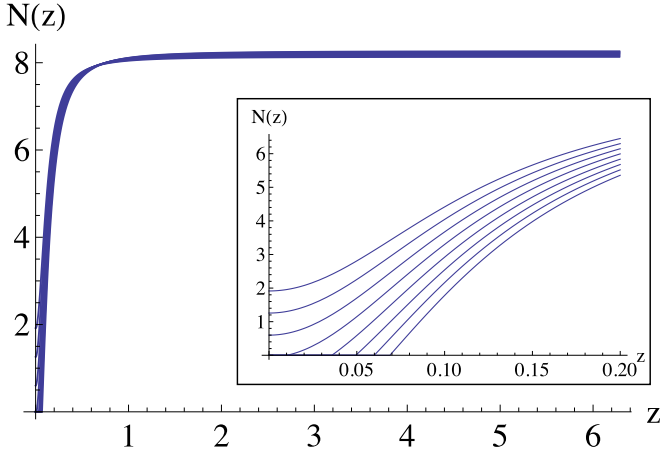


FIG. 5. (Color online) Behavior of the energy density $N(z)$ for $\kappa = 0.9$, $\mu = 0.8$, $E = 8$ and N ranging in steps of 0.1 from top to bottom from 0.5 to 1.2, near to the critical temperature $N_{\text{crit}} \sim 0.8$. As expected, $N(z)$ is always increasing. If we exclude the region near $z = 0$, the functions are almost identical and approach nearly the same constant value for $z \gtrsim 1$. Inset: Zoom on the region $z \rightarrow 0$. We can see that above the critical temperature $N(z)$ is zero on a finite interval, while below it $N(z)$ approaches a positive value which strongly depends on the temperature.

The behavior of $N(z)$ in the amplifier case is shown in Fig. 6. It is completely analogous to the thermal attenuator, but for our choice of the parameters ($\kappa = 1.1$, $\mu = 0.8$, $E = 8$) the critical temperature is much greater, $N_{\text{crit}} \sim 9.8$.

An analysis of the fraction $\frac{z_0}{2\pi}$ (remember that z_0 ranges from 0 to 2π) of the unused beam splitters is presented in Fig. 7. For fixed κ and μ , for zero temperature ($N = 0$) all the beam splitters are exploited and $z_0 = 0$; then z_0 remains zero

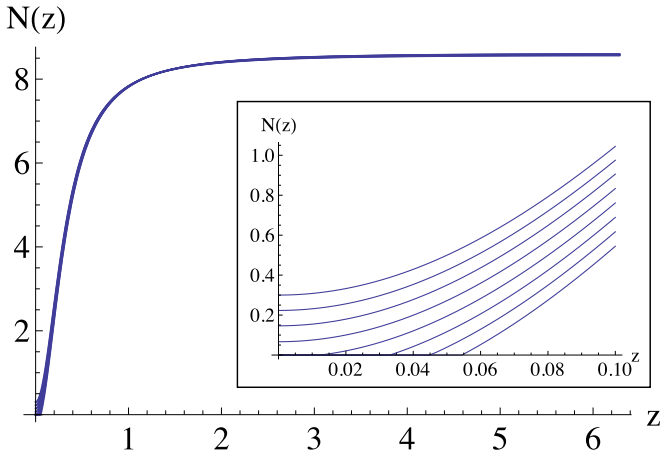


FIG. 6. (Color online) Behavior of the energy density $N(z)$ for $\kappa = 1.1$, $\mu = 0.8$, $E = 8$ and N ranging in steps of 0.1 from top to bottom from 9.4 to 10.1, near to the critical temperature $N_{\text{crit}} \sim 9.8$. As expected, $N(z)$ is always increasing. If we exclude the region near $z = 0$, the functions are almost identical and approach nearly the same constant value for $z \gtrsim 1$. Inset: Zoom on the region $z \rightarrow 0$. We can see that above the critical temperature $N(z)$ is zero on a finite interval, while below it $N(z)$ approaches a positive value which strongly depends on the temperature.

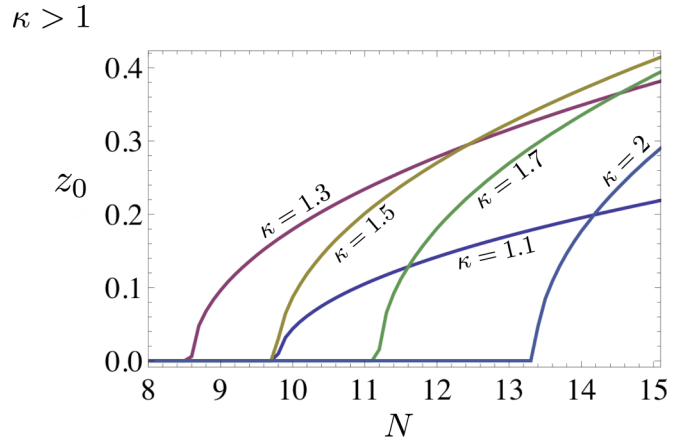
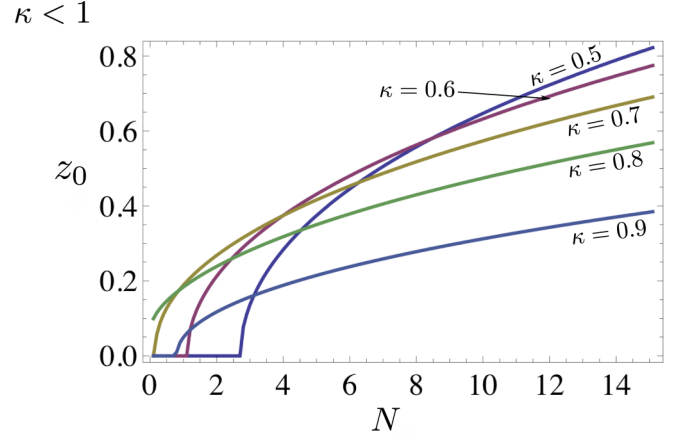


FIG. 7. (Color online) Behavior of the fraction $\frac{z_0}{2\pi}$ (z_0 ranges from 0 to 2π) of unused beam splitters as a function of the temperature N for $E = 8$, $\mu = 0.8$, and various values of κ . At zero temperature ($N = 0$) all the beam splitters are exploited and $z_0 = 0$; then z_0 remains zero up to the critical temperature N_{crit} , and grows for $N > N_{\text{crit}}$. We notice that for typical values of the parameters N_{crit} is much greater for $\kappa > 1$ than for $0 < \kappa < 1$. In the infinite temperature limit $N \rightarrow \infty$ only an infinitesimal fraction of the beam splitters is used and z_0 tends to 2π , even if this is not evident from the plots due to the limited range of N .

up to the critical temperature N_{crit} , and grows for $N > N_{\text{crit}}$. We can notice that for typical parameters, the critical value N_{crit} for the beam splitter is much lower than for the amplifier.

We will now show that in the infinite temperature limit ($N \rightarrow \infty$), z_0 tends to 2π , and the optimal configuration concentrates all the energy on an infinitesimal fraction of the beam splitters. First, notice that for $N \rightarrow \infty$ the multiplier λ in (71) must tend to zero, and we can approximate $e^{\lambda/\eta} - 1 \sim \lambda/\eta$, getting

$$N(z) = \left[\frac{1}{\lambda} - \left(\frac{1}{\eta(z)} - 1 \right) N \right] \theta(z - z_0) + O(1), \quad (72)$$

where z_0 is the point where $N(z)$ vanishes, given by

$$\frac{1}{\lambda} = \left(\frac{1}{\eta(z_0)} - 1 \right) N. \quad (73)$$

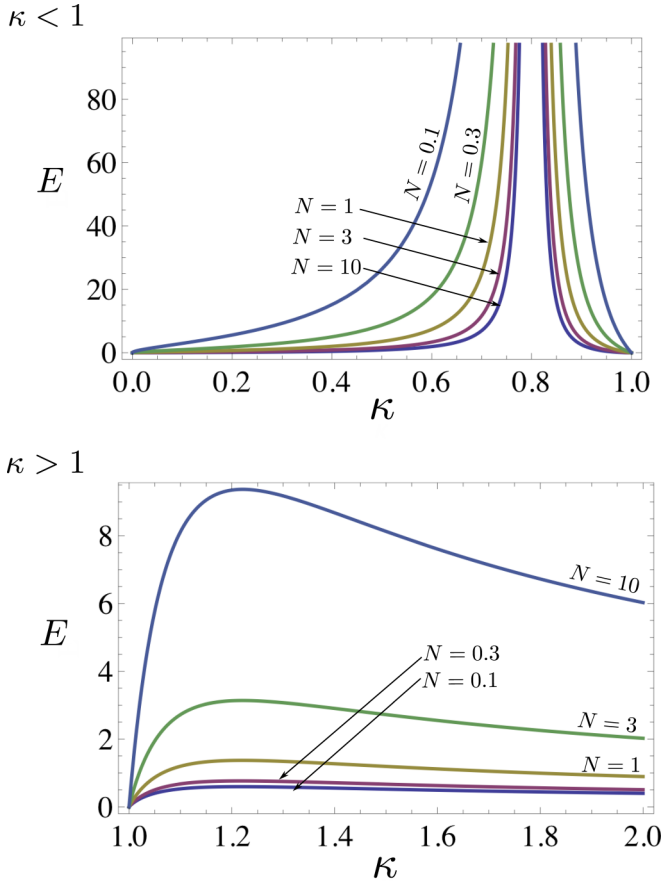


FIG. 8. (Color online) Behavior of the minimal energy for which all the beam splitters are exploited as a function of κ for $\mu = 0.8$ and various values of the temperature N . As expected, E grows with the temperature, and $E = 0$ for $\kappa = 0, 1$ and $\kappa \rightarrow \infty$. In the attenuator case we notice the divergence of E for $\kappa = \mu (= 0.8)$, due to the fact that $\eta(0) = 0$ and for any positive temperature the optimal $N(z)$ must vanish on a finite interval.

The energy constraint (38) can be now written as

$$E = N \int_{z_0}^{2\pi} \left(\frac{1}{\eta(z_0)} - \frac{1}{\eta(z)} \right) \frac{dz}{2\pi} + O(1), \quad (74)$$

and since $\eta(z)$ is strictly increasing, the only way to keep E finite for $N \rightarrow \infty$ is to let $z_0 \rightarrow 2\pi$, i.e., in the high temperature limit all the energy is concentrated on an infinitesimal fraction of the beam splitters.

The minimum energy E_{crit} for which all the beam splitters are exploited is shown in Fig. 8 for various values of the temperature N . We know that for $\kappa = 0, 1$ and $\kappa \rightarrow \infty$

no beam splitter is left unused, and indeed $E_{\text{crit}} = 0$ at these points. As expected, E_{crit} always grows with the temperature. In the attenuator case, we notice a divergence of E_{crit} for $\kappa = \mu$ ($\mu = 0.8$ in the plot). Actually, if $\kappa = \mu$ we have $\eta(0) = 0$ [while in any other case $\eta(z)$ is always positive], and some normal modes have infinitesimal transmissivity. It is then natural that for any nonzero temperature it is not convenient to send energy into these low-capacity modes. More formally, the argument of the positive part in (71) in the case $\kappa = \mu$ in $z = 0$ is $-N < 0$, so for any $N > 0$ the positive part must be taken into account.

V. CONCLUSIONS

In this work we study a model of Gaussian thermal memory channels extending a previous proposal by Lupu *et al.* [21,22] in order to incorporate the disturbance of thermal noise. The memory effects imply that successive uses of a channel cannot be considered independently but they are potentially correlated [15,16]. In our model this correlation is generated by an internal memory mode which is assumed to be inaccessible by the users of the channel.

Exploiting the factorization into independent normal modes [22] and a recent breakthrough in the theory of memoryless channels [10], we explicitly determine the classical capacity of our memory channel model. We find that, as in the memoryless case, coherent states are sufficient for an optimal coding. However, the associated probability distribution is factorized only in the normal mode decomposition that diagonalizes the channel, so in order to fully exploit its intrinsic memory, the input signals $\{a_j\}$ (and consequently their outputs counterparts) must be correlated. Then the optimal transmission rate of information can still be achieved by independent uses of the channel, but the probability distribution of the physical inputs will not be factorized.

Our results can find applications in bosonic communication channels with memory effects and affected by a non-negligible amount of thermal noise. In particular, low frequency communication devices, e.g., GHz communication systems [29], THz lasers [30], etc., are intrinsically subject to blackbody thermal noise and thus they fall in the theoretical framework presented in this work.

ACKNOWLEDGMENTS

The authors are grateful to C. Lupu and S. Mancini for useful comments. G.d.P. thanks A. Tomadin for comments and discussions. This work is partially supported by the EU Collaborative Project TherMiQ (grant agreement 618074).

- [1] C. M. Caves and P. B. Drummond, *Rev. Mod. Phys.* **66**, 481 (1994).
 [2] A. S. Holevo, *Quantum Systems, Channels, Information: A Mathematical Introduction* (De Gruyter, Berlin/Boston, 2012).

- [3] A. S. Holevo and R. F. Werner, *Phys. Rev. A* **63**, 032312 (2001).
 [4] B. Schumacher and M. D. Westmoreland, *Phys. Rev. A* **56**, 131 (1997).
 [5] S. L. Braunstein and P. van Loock, *Rev. Mod. Phys.* **77**, 513 (2005).

- [6] J. Eisert and M. M. Wolf, *Quantum Information with Continuous Variables of Atoms and Light* (Imperial College Press, London, 2007), pp. 23–42.
- [7] C. Weedbrook, S. Pirandola, R. García-Patrón, N. J. Cerf, T. Ralph, J. H. Shapiro, and S. Lloyd, *Rev. Mod. Phys.* **84**, 621 (2012).
- [8] V. Giovannetti, A. S. Holevo, and R. García-Patrón, [arXiv:1312.2251](https://arxiv.org/abs/1312.2251) [Commun. Math. Phys. (to be published)].
- [9] A. Mari, V. Giovannetti, and A. S. Holevo, *Nat. Commun.* **5**, 3826 (2014).
- [10] V. Giovannetti, R. García-Patrón, N. J. Cerf, and A. S. Holevo, *Nat. Phot.* **8**, 796 (2014).
- [11] B. R. Bardhan, R. García-Patrón, M. M. Wilde, and A. Winter, [arXiv:1401.4161](https://arxiv.org/abs/1401.4161).
- [12] F. Caruso, V. Giovannetti, C. Lupo, and S. Mancini, [arXiv:1207.5435](https://arxiv.org/abs/1207.5435) [Rev. Mod. Phys. (to be published)].
- [13] K. Banaszek, A. Dragan, W. Wasilewski, and C. Radzewicz, *Phys. Rev. Lett.* **92**, 257901 (2004); R. Demkowicz-Dobrzański, P. Kolenderski, and K. Banaszek, *Phys. Rev. A* **76**, 022302 (2007).
- [14] E. Paladino, L. Faoro, G. Falci, and R. Fazio, *Phys. Rev. Lett.* **88**, 228304 (2002); Y. Hu, Y.-F. Xiao, Z.-W. Zhou, and G.-C. Guo, *Phys. Rev. A* **75**, 012314 (2007).
- [15] R. G. Gallager, *Information Theory and Reliable Communication* (Wiley, New York, 1968).
- [16] D. Kretschmann and R. F. Werner, *Phys. Rev. A* **72**, 062323 (2005).
- [17] N. Datta and T. C. Dorlas, *J. Phys. A: Math. Theor.* **40**, 8147 (2007); A. D’Arrigo, G. Benenti, and G. Falci, *New J. Phys.* **9**, 310 (2007).
- [18] V. Giovannetti, *J. Phys. A* **38**, 10989 (2005).
- [19] V. Giovannetti and S. Mancini, *Phys. Rev. A* **71**, 062304 (2005).
- [20] N. J. Cerf, J. Clavareau, C. Macchiavello, and J. Roland, *Phys. Rev. A* **72**, 042330 (2005).
- [21] C. Lupo, V. Giovannetti, and S. Mancini, *Phys. Rev. Lett.* **104**, 030501 (2010).
- [22] C. Lupo, V. Giovannetti, and S. Mancini, *Phys. Rev. A* **82**, 032312 (2010).
- [23] O. V. Pilyavets, C. Lupo, and S. Mancini, *IEEE Trans. Inf. Theory* **58**, 6126 (2012).
- [24] J. Schäfer, D. Daems, E. Karpov, and N. J. Cerf, *Phys. Rev. A* **80**, 062313 (2009).
- [25] J. Schäfer, E. Karpov, and N. J. Cerf, *Phys. Rev. A* **84**, 032318 (2011); **85**, 012322 (2012).
- [26] C. Lupo, L. Memarzadeh, and S. Mancini, *Phys. Rev. A* **80**, 042328 (2009).
- [27] N. Gisin, G. Ribordy, W. Tittel, and H. Zbinden, *Rev. Mod. Phys.* **74**, 145 (2002).
- [28] S. Tanzilli, W. Tittel, H. De Riedmatten, H. Zbinden, P. Baldi, M. DeMicheli, D. B. Ostrowsky, and N. Gisin, *Eur. Phys. J. D* **18**, 155 (2002).
- [29] C. Lang, C. Eichler, L. Steffen, J. M. Fink, M. J. Woolley, A. Blais, and A. Wallraff, *Nat. Phys.* **9**, 345 (2013).
- [30] R. Köhler, A. Tredicucci, F. Beltram, H. E. Beere, E. H. Linfield, A. G. Davies, D. A. Ritchie, R. C. Iotti, and F. Rossi, *Nature (London)* **417**, 156 (2002).
- [31] V. W. S. Chan, *J. Lightw. Technol.* **24**, 4750 (2006); A. Fedrizzi, R. Ursin, T. Herbst, M. Nespoli, R. Prevedel, T. Scheidl, F. Tiefenbacher, T. Jennewein, and A. Zeilinger, *Nat. Phys.* **5**, 389 (2009).
- [32] R. M. Gray, *Toeplitz and Circulant Matrices: A Review* (Now Publishers, Norwell, MA, 2006).